

# Lateral crystallite size and lattice distortions in cellulose II samples of different origin

D. Hofmann, H.-P. Fink and B. Philipp

Academy of Sciences of the GDR, Institute of Polymer Chemistry 'Erich Correns', 1530 Teltow-Seehof, GDR

(Received 1 March 1988; revised 20 June 1988; accepted 11 July 1988)

On the basis of wide-angle X-ray scattering measurements on seven cellulose II samples of different origin, the effects of finite crystallite size and lattice distortions on the linewidth of the (10 1) reflection are discussed. In this context the paracrystal model and the microstrain concept are compared and a single-line technique recently published is employed. Separate determinations of lateral crystallite size and lattice distortion parameters are given for the first time for cellulose II samples. The lateral crystallite size distribution was found to be rather narrow in each of the samples. The crystallite sizes obtained were between 3.3 and 5.8 nm and the corresponding root-mean-square strains were between 0.034 and 0.025. The contribution of lattice distortions to the total linewidth does not exceed 10%, thus showing the order of magnitude of deviation that has to be taken into account in employing the Scherrer equation for crystallite size determination and neglecting lattice distortions.

(Keywords: cellulose II; wide-angle X-ray scattering; reflex profile analysis; single-line method)

## INTRODUCTION

Crystallite size is an essential parameter in characterizing the physical structure of cellulose as a partially crystalline polymer. Lateral crystallite size (*LCS*), i.e. the average diameter of the ordered regions perpendicular to the chain direction, can greatly influence the chemical processing of cellulose, such as for example during alkalization<sup>1-3</sup>. With regard to viscose rayon manufacture, *LCS* depends significantly on the process parameters, on the one hand, and on the other hand the dimensions of the predominantly axially oriented crystallites are an important factor in determining the textile properties of viscose rayon filaments and staples<sup>4</sup>. *LCS* is frequently determined by measuring the halfwidth of reflections in the wide-angle X-ray scattering (WAXS) pattern<sup>1-12</sup>. But in this connection, the often neglected influence of lattice distortions on WAXS peak broadening and on crystallite size determination should be considered.

Up to now, crystallite sizes and lattice distortions of cellulose have been obtained separately only along the chain direction. This was performed on the basis of the paracrystal concept<sup>8-12</sup>, employing higher-order reflections of the (0 10) lattice planes for the analysis. These results also led to the indirect assumption that in determining *LCS* via WAXS peak halfwidth the deviation due to lattice distortions does not exceed 10%<sup>2-4</sup>. A direct and separate estimation of *LCS* and lattice distortions from the shape of equatorial reflections has so far not been considered possible, as only first-order reflections are visible in the WAXS pattern and suitable single-line methods were not available (cf. ref. 13).

Quite recently, a single-line method based on the microstrain model for separating *LCS* and lattice distortions was published by us<sup>14</sup>. This method is applied

in this paper to cellulose II samples of different origin. This direct separate determination of lateral crystallite size and lattice distortion parameters is applied to cellulose II samples for the first time. The results are compared with those obtained with the paracrystal model<sup>9-12</sup>. For one of our samples also the relation between lattice distortions determined here and the crystalline disorder parameter *k* calculated previously<sup>2</sup> according to Ruland<sup>15</sup> and Vonk<sup>16</sup> is discussed.

Furthermore this investigation aims to give an idea of the influence of lattice distortions on WAXS line broadening in general.

## EXPERIMENTAL PROCEDURE AND DATA TREATMENT

### Cellulose samples

The samples investigated were characterized in Table 1. Most of them (B, C, D) are commercial rayon staple fibre samples, especially of the high-wet-modulus (HWM) type (B-1 to B-4). Samples C and D are normal-grade viscose staple fibres and viscose filaments, respectively. The HWM-type samples differ somewhat in their textile properties. The alkali-treated and subsequently regenerated cotton linters sample A was analysed earlier in connection with alkali cellulose formation<sup>2</sup> by the Ruland-Vonk method<sup>15,16</sup>. For this sample the degree of crystallinity was  $x_c = 0.43-0.48$  and the lattice disorder parameter was  $k = 2.1 \times 10^{-2}$  to  $2.4 \times 10^{-2} \text{ nm}^2$ .

For further characterization, the cuprammonium *DP* and the level-off *DP* of our samples were determined. The values of these parameters increased in the order: normal-grade fibres, HWM-type fibres and slack mercerized cotton linters, probably indicating different super-molecular structures in the chain direction.

**Table 1** Characterization of samples

Sample	Origin/preparation	DP <sub>Cu</sub>	LODP	Tenacity (mN/tex)		Loop tenacity (mN/tex)	Wet modulus (mN/tex)	Elongation at break (%)	
				Dry	Wet			Dry	Wet
A	Linters, mercerized	1167	82	—	—	—	—	—	—
B-1	HWM viscose staple	307	60	333	192	72	989	16	16
B-2	HWM viscose staple	330	—	335	218	67	1296	14	18
B-3	HWM viscose staple	304	49	333	243	75	1100	15	17
B-4	HWM viscose staple	307	54	364	247	83	753	19	24
C	Normal-grade viscose staple fibre	264	37	200	115	66	515	19	24
D	Normal-grade viscose filament	261	38	—	—	—	—	—	—

### WAXS measurements

A horizontal X-ray counter diffractometer HZG 4-A (Freiberger Präzisionsmechanik Freiberg/S., GDR) was used in symmetric transmission mode, employing Ni-filtered Cu K<sub>α</sub> radiation ( $\lambda = 0.15418$  nm) and an impulse height analyser with stepwise recording in the angular range  $4^\circ \leq 2\theta \leq 40^\circ$  at a step width of  $0.1^\circ$ . Oriented fibre samples were positioned with their fibre axis perpendicular to the goniometer plane. With a measuring time of 120 s for each step the statistical error was less than 1% in impulse counting. The registered data were corrected with regard to parasitic scattering, absorption and polarization. Additionally a numerical correction for K<sub>α1,α2</sub> doublet broadening according to Keating<sup>17</sup> was applied. The result was a scattering intensity curve  $I(s)$  with  $s = (2 \sin \theta)/\lambda$ .

### Processing and evaluation of data

The single-line technique<sup>14</sup>, which is highly sensitive to the shape of the WAXS peak profile, can be applied with high accuracy especially to the (101) reflection (notation according to Meyer and Misch<sup>18</sup>) as this peak is resolved distinctly in the pattern. Therefore only this WAXS profile was further treated.

Separation of background scattering as a prerequisite for WAXS peak profile analysis was performed via an  $Is^2$  vs.  $s$  plot (cf. also Figure 1). A certain amount of cellulose IV modification was noticed for HWM-type fibres only. For the purposes of smoothing the reflection profile, before determining the integral width and the WAXS peak profile type (Gaussian or Cauchy), a Pearson-VII function was subsequently fitted to the (101) reflection profile<sup>19</sup>:

$$P(s) = I_{\max} [1 + 4\tilde{\beta}^{-2}(2s - s_{\max})^2(2^{1/m} - 1)]^{-m} \quad (1)$$

with  $I_{\max}$  = maximum intensity,  $\tilde{\beta}$  = halfwidth of the WAXS peak,  $s$  = amount of scattering vector and  $s_{\max}$  = position of the maximum of the WAXS reflection. Using the parameter  $m$  the shape of the curve can be varied within wide limits, e.g. for Cauchy shape  $m = 1$  and for Gaussian shape  $m \rightarrow \infty$ .

Finally, the peak profiles were corrected according to the work of Stokes<sup>20</sup> for instrumentally induced broadening, employing an anthracene sample as a standard. As a result of this procedure, the Fourier transform cosine coefficients  $A_n$  of the appropriate WAXS reflection profiles were obtained with a residual broadening resulting only from structural parameters of the cellulose sample.

For comparison of the method formerly used in the literature and the new single-line technique of LCS

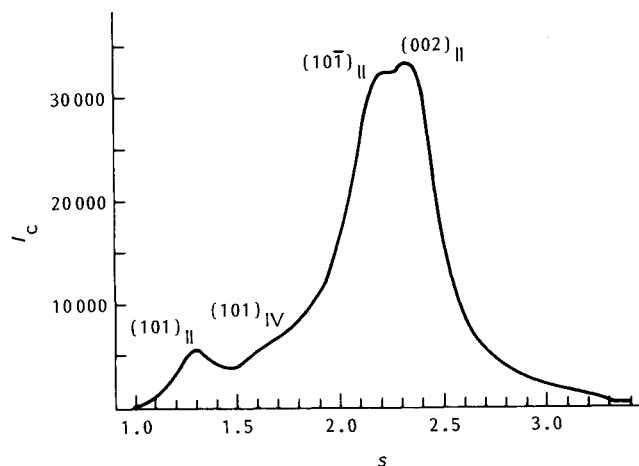


**Figure 1** Equatorial WAXS of sample B-2 with background separation:  $I_c$  = intensity of crystalline reflections;  $s$  = scattering variable

determination, we started from the well known Scherrer equation correlating reflection broadening and crystallite size. The Pearson-VII function fitted to the (101) peak profile provides the integral linewidth  $\beta$ , from which a minimum weight-averaged crystallite size  $H_{101} = 1/\beta$  was calculated. This value of  $H_{101}$  is not corrected for instrumental broadening nor for lattice distortions. But based on plausible assumptions these corrections can be made. The experimental WAXS profile is a convolution of the measurable instrumental broadening  $I_i(s)$  and the sample structure-related broadening. This latter broadening in turn is a convolution of  $I_d(s)$  due to lattice distortions and  $I_s(s)$  due to finite crystallite size. Assuming a Gaussian shape for all these partial profiles, then:

$$\beta_s = (\beta^2 - \beta_i^2 - \beta_d^2)^{1/2} \quad (\text{rad}) \quad (2)$$

holds true for the completely corrected integral linewidth  $\beta_s$  (note that  $\beta_s(\text{rad}) = \beta_s(\text{nm}^{-1})\lambda/\cos \theta$ ). Using a Gaussian profile again the unknown integral width  $\beta_d$  can be calculated from the local root-mean-square lattice strain  $\langle e_0^2 \rangle^{1/2}$  value<sup>13</sup> obtained by a single-line technique<sup>14</sup>:

$$\beta_d = \sqrt{\langle e_0^2 \rangle} 2(2\pi)^{1/2} \tan \theta_{\max} \quad (\text{rad}) \quad (3)$$

With  $\beta$ ,  $\beta_i$  and  $\beta_d$  known,  $\beta_s$  can be calculated, and using the Scherrer equation the fully corrected 'true' average crystallite size  $\hat{H}_{101}$  can be obtained. To characterize the difference between  $H_{101}$  and  $\hat{H}_{101}$  a parameter  $K = (\hat{H}_{101} - H_{101})/\hat{H}_{101}$  was used.

In order to separate the effects of LCS and lattice distortions we employed a method based on Fourier

analysis of a single WAXS reflection. Using appropriate approximations for  $A_n^s$  and  $A_n^d$  the following relation between the Fourier cosine coefficients  $A_n$  and some structure-related parameters can be obtained<sup>14</sup>:

$$A_n = A_0 [1 - n/N_3 - 2\pi^2 r^2 \langle e_0^2 \rangle n^2 + (2\pi^2 r^2 \langle e_0^2 \rangle / N_3 - 2\pi^2 r^2 \langle ee' \rangle) n^3] \quad (4)$$

with  $n$  being the Fourier order and  $r$  being the order of the investigated WAXS reflection.  $N_3$  can be understood using the column cell model of Warren and Averbach<sup>21</sup>. According to this model each of the crystallites is divided into columns perpendicular to the scattering lattice planes with each column composed of cells with an average height  $d$ . Then  $N_3$  denotes the mean number of cells perpendicular to the  $(hkl)$  planes in one crystallite averaged over all the columns and all the crystallites. The number average of the crystallite size  $L_{hkl}$  is then obtained by multiplication of  $N_3$  by the cell height  $d$  (cf. ref. 14).

The average  $\langle e_0^2 \rangle$  is the local mean-squared lattice strain from which  $\langle e_1^2 \rangle$ , the common mean-squared lattice strain, can be obtained:

$$\langle e_1^2 \rangle = \langle e_0^2 \rangle + \langle ee' \rangle \approx \langle e_0^2 \rangle \quad (5)$$

Fitting now a third-order polynomial in the Fourier order  $p_n = a_0 + an + bn^2 + cn^3$  to the Fourier cosine coefficients of an experimental WAXS peak profile the structural parameters in question can be obtained by comparison of the coefficients according to equations (6)–(9):

$$A_0 = a_0 \quad (6)$$

$$N_3 = -a_0/a \quad (7)$$

$$\langle e_0^2 \rangle = -b/(2\pi^2 r^2 a_0) \quad (8)$$

$$\langle ee' \rangle = \langle e_0^2 \rangle / N_3 - c/(2\pi^2 r^2 a_0) \quad (9)$$

For further details the reader is referred to ref. 14.

## RESULTS AND THEIR PHENOMENOLOGICAL INTERPRETATION

The results of the (101) reflection profile analysis are listed in Table 2 for the cellulose II samples investigated here. For a better understanding of the following discussion, the parameters given may be briefly considered. Smoothing the (101) peak profile by fitting a

Pearson-VII function gives the halfwidth  $\beta$  and the form parameter  $m$ , by means of which the integral linewidth  $\beta$  can be calculated. Because of the high values of  $m \geq 6$  the WAXS reflection profiles of our samples can be considered nearly Gaussian. The instrumental broadening as obtained using an anthracene standard specimen is also of Gaussian shape ( $m=20$ ) and corresponds to an integral linewidth of  $\beta_i = 0.00403$  (rad). The weight-averaged LCS obtained from  $\beta$  are between 3.6 and 5.1 nm. The deviation between  $H_{101}$  and the corrected values  $\hat{H}_{101}$  did not much exceed 10%. The LCS  $L_{101}$  obtained from the Fourier coefficients represent number averages. They varied between 3.3 and 5.8 nm and decreased in the order: mercerized linters > HWM viscose staple > normal-grade viscose rayon. The small differences between the number averages  $L_{101}$  and the corresponding weight averages  $\hat{H}_{101}$  indicate a narrow distribution of crystallite sizes in the cellulose II samples irrespective of their origin (cf. Table 1).

The course of LCS variation correlates quite well with that of the level-off DP, clearly indicating some coherence between lateral and longitudinal ordering in cellulose II samples. In spite of significant differences in LCS of the HWM-type samples B-1 to B-4 a simple direct correlation of these values and textile properties could not be derived.

There are probably further structural features including other structural levels (e.g. fibrillar morphology<sup>4</sup>) determining the textile properties in a rather complex way.

The large LCS of mercerized linters as compared to the different rayon samples can be traced back to the high LCS of native linters, which has been determined previously<sup>2,3</sup> to be 4.7 nm. As also shown in these papers, mercerization leads to a dissolution of smaller crystallites and a breakdown of bigger ones. This obviously produces the very narrow distribution of cellulose II crystallite sizes as demonstrated by the nearly identical values of  $\hat{H}_{101}$  and  $L_{101}$  in Table 2.

Our LCS data are in good agreement with those of Haase *et al.*<sup>9-12</sup>, who published values for the  $LCS_{101}$  of 4.7 nm for Tufcel<sup>R</sup> and 5.7 nm for Fortisan<sup>R</sup>. The root-mean-square strain  $\langle e_1^2 \rangle^{1/2}$  of our samples amounted to about 3% with a tendency to increase with decreasing LCS.

## GENERAL DISCUSSION

The following discussion is centred on a comparison of the microstrain model<sup>21,22</sup> and the paracrystal model<sup>23</sup> as the theoretical basis for separating crystallite size and lattice distortion effects in the analysis of WAXS peak

**Table 2** Results of the WAXS profile analysis concerning the (101) reflection of different cellulose II samples

Sample	Integral linewidth, $\beta$ (nm <sup>-1</sup> )	Half linewidth, $\beta$ (nm <sup>-1</sup> )	Shape parameter, $m$	LCS from $\beta$ , $H_{101}$ (nm)	True weight-average LCS, $\hat{H}_{101}$ (nm)	$K = (\hat{H}_{101} - H_{101})/\hat{H}_{101}$	True number average LCS, $L_{101}$ (nm)	Root-mean-squared strain, $\langle e_1^2 \rangle^{1/2}$	Hosemann parameter, $\alpha^*$	Ruland parameter, $k \times 10^2$ (nm <sup>2</sup> )
A	0.197	0.185	12.5	5.1	5.9	0.137	5.8	0.027	0.078	0.52
B-1	0.218	0.198	6.5	4.6	5.1	0.091	4.8	0.025	0.066	0.44
B-2	0.218	0.198	6.0	4.6	5.0	0.091	4.7	0.026	0.067	0.45
B-4	0.254	0.230	6.0	3.9	4.4	0.097	3.8	0.030	0.075	0.66
B-3	0.259	0.233	8.0	3.9	4.2	0.084	3.9	0.031	0.074	0.67
D	0.266	0.244	9.0	3.8	4.2	0.098	3.7	0.032	0.077	0.74
C	0.281	0.255	6.5	3.6	3.9	0.095	3.3	0.034	0.078	0.80

profiles of the (101) reflection of cellulose II. The microstrain model is valid for slightly distorted crystallites only. But also in this case both concepts are usually regarded as competitive<sup>23,25-27</sup>.

One major point of consideration is the correlation between peak broadening and peak order. In the literature it is often assumed that in the case of a paracrystalline material the integral linewidth of a WAXS reflection broadened only by lattice distortions increases with increasing square of the reflection order  $r$ . In the case of microstrain lattice distortions, however, a linear relationship is assumed to exist (cf. ref. 23, 25-27). In this connection some critical comment seems to be necessary.

A quadratic dependence of linewidth on peak order requires in the paracrystal case the distance statistics  $H_i(x)$  to be of the Gaussian type. This prerequisite is generally met in Hosemann's work. On the other hand, for the derivation of the linear relationship in the case of the microstrain model, the following approximation is usually applied to the Fourier cosine coefficients  $A_n^d$  of a WAXS profile depending on lattice distortions only<sup>25</sup>:

$$A_n^d = \exp(-2\pi^2 r^2 n^2 \langle e_n^2 \rangle) \quad (10)$$

with  $\langle e_n^2 \rangle$  being the mean-squared strain of  $n$ th order. (Note that this assumption is exactly valid only if a Gaussian distribution is assumed for these lattice strain variables<sup>25</sup>.)

Furthermore, the following equation holds for the integral linewidth  $\beta_d$  of a WAXS reflection broadened by lattice distortions only<sup>25</sup>:

$$\beta_d \sim 1 \left/ \sum_{n=-\infty}^{\infty} A_n^d \right. \quad (11)$$

With the sum being approximated by an integral, we obtain with (10) the equation<sup>26</sup>:

$$\beta_d \sim 1 \left/ \sum_{-\infty}^{+\infty} \exp(-2\pi^2 r^2 n^2 \langle e_n^2 \rangle) dn \right. \quad (12)$$

Thus, the functional dependence of  $\beta_d$  on the reflection order is decisively related to the course of the mean-squared lattice strain  $\langle e_n^2 \rangle$  with the Fourier order  $n$ . The relation usually applied in the literature,  $\beta_d \sim r$ , is thus based on the assumption  $\langle e_n^2 \rangle = \langle e_1^2 \rangle = \text{constant}$ .

In this case the relation:

$$\beta \sim r(2\pi \langle e_1^2 \rangle)^{1/2} \quad (13)$$

holds true (cf. ref. 26). But it should be stressed that the assumption  $\langle e_n^2 \rangle = \text{constant}$  is valid only in relatively few special cases. However, taking a hyperbolic relation  $\langle e_n^2 \rangle = \langle e_1^2 \rangle / n$  for example, as was shown to be rather useful for some metallic samples<sup>28,29</sup>, we arrive at:

$$\beta_d \sim 2\pi^2 r^2 \langle e_1^2 \rangle \quad (14)$$

i.e. at a quadratic relation between reflection width and reflection order. Thus, the dependence of WAXS peak width  $\beta_d$  on peak order can obviously be modelled by functional relations of different kinds within the framework of the microstrain concept. From this discussion it may be concluded that the microstrain model is more versatile with regard to all possible

functional relations  $\beta_d = f(r)$ . Consequently it is of more general applicability than the paracrystal model in describing the influence of lattice distortions on a WAXS pattern for only slightly disordered crystalline regions.

On the basis of this theoretical background a more detailed comparison of our results obtained by the single-line techniques and some results of Hosemann *et al.* seems to be useful. Generally, a remarkably good compatibility of these data can be stated. The nearly Gaussian profiles of the cellulose II (101) reflections concluded from the shape parameters  $m$  of the Pearson-VII function fitting (cf. Table 2) have also been found by Hosemann *et al.* using a Guinier plot<sup>10,12</sup>. The indirect estimation of a lateral lattice distortion parameter  $g_{101}$  published in refs. 15 and 30 on the basis of axial  $g_{010}$  and  $\alpha_{010}^*$  parameters for two cellulose II samples, Tufcel<sup>R</sup> and Fortisan<sup>R</sup>, covers the same range of 0.03 to 0.04 as calculated for the root-mean-square lattice strain  $\langle e_1^2 \rangle^{1/2}$  of the cellulose II samples investigated here. As already mentioned, our  $H_{101}$  values of the crystallite size perpendicular to the (101) lattice planes of 3.6-5.1 nm (uncorrected values) are quite compatible with the corresponding data of Haase *et al.*<sup>10,11</sup> (4.7 nm for Tufcel<sup>R</sup> and 5.7 nm for Fortisan<sup>R</sup>).

The data of lattice distortions and crystallite size parameters presented in Table 2 can also be used for determining the true LCS  $\hat{H}_{101}$  using formulae (2) and (3). Furthermore it is possible to estimate the expected maximum deviation between  $\hat{H}_{101}$  and  $H_{101}$ . It has to be mentioned that in all cases the correction concerning instrumental broadening is negligible in comparison with the lattice distortion correction. The relative difference between uncorrected and true LCS denoted by  $K$  (cf. Table 2) can therefore be related almost completely to lattice distortions with the  $K$  values generally not exceeding 10%. This again is in really good agreement with the indirect estimation of Haase *et al.*<sup>9</sup> on the basis of the axial  $\alpha_{010}^*$  parameter, defined by the equation:

$$\alpha_{010}^* = g_{010}(H_{010}/d_{010})^{1/2} \quad (15)$$

According to an empirical statement of Hosemann<sup>24</sup> this parameter is some kind of material constant for a certain class of materials. (This means from the physical point of view that the maximum crystallite size obtainable is limited by the amount of lattice distortions.) Indeed, our  $\alpha_{101}^* = (\langle e_1^2 \rangle_{101} L_{101}/d_{101})^{1/2}$  values calculated for rather different cellulose II specimens on the basis of the microstrain concept show a remarkable constancy. Its amount of  $\approx 0.8$  agrees pretty well with the data given in ref. 9 of  $\alpha_{010}^*$  in the chain direction for two cellulose II samples, i.e.  $\alpha_{010}^* = 0.07$  for Tufcel<sup>R</sup> and  $\alpha_{010}^* = 0.10$  for Ramie<sup>R</sup>. A larger difference, however, does exist between our  $\alpha_{101}^*$  data presented in Table 2 for cellulose II and the value of  $\alpha_{101}^* = 0.13$  for the lateral direction in cellulose II published by Hosemann *et al.*<sup>30</sup> without further comments on the procedure of its determination.

Finally, the relation between the lattice distortion parameters so far discussed and the crystalline disorder parameter  $k$  according to Ruland<sup>15</sup> will be considered. *A priori*, this  $k$  parameter can comprise first- and second-order lattice distortions as  $k$  is determined by the scattering-angle-dependent damping  $D$  of crystalline

WAXS reflections of polymers, according to<sup>15</sup>:

$$D = \exp(-2ks^2) \quad (16)$$

with

$$k = k_T + k_1 + k_2 \quad (17)$$

The term  $k_T$  denotes thermal lattice vibrations, and  $k_1$  and  $k_2$  represent first- and second-order lattice distortions, respectively;  $k_2$  can be estimated from Hosemann's  $g$  parameter or from the mean-squared lattice strain  $\langle e_1^2 \rangle$  according to<sup>31</sup>:

$$k_2 = 1.4\pi^2 \langle e_1^2 \rangle d^2 \quad (18)$$

For our cellulose sample (alkalized and subsequently neutralized linters) the  $k_2$  value of  $0.52 \times 10^{-2} \text{ nm}$  estimated by equation (18) can be compared to Ruland's  $k$  parameter determined previously<sup>2,3</sup> to be in the range  $(2.1-2.4) \times 10^{-2} \text{ nm}^2$ . Second-order lattice distortions obviously are not the main source for the damping  $D$  or the damping exponent  $k$  here. This is in agreement with publications of other groups<sup>31</sup> pointing out that with polymers at room temperature the thermal lattice vibrations are the dominating factor in determining  $k$ .

## CONCLUSIONS

Summarizing the experimental results and the considerations presented here, the following major conclusions may be drawn:

Both the microstrain and the paracrystal concepts are adequate and suitable theoretical models for analysing lateral reflection profiles in the WAXS pattern of cellulose II of different origin. The corresponding structural parameters show a remarkably good compatibility.

Assuming a sufficiently narrow instrumental broadening function, the linewidth of lateral WAXS reflections of cellulose II samples originates to a very high extent from finite crystallite size effects. This means that LCS determination of cellulose by making use of linewidth measurements and the Scherrer equation and neglecting the influence of lattice distortions arrives at averaged values with maximum  $-10\%$  deviation from the true LCS. These results confirm earlier studies based on the paracrystalline concept<sup>9</sup> as well as support earlier LCS measurements<sup>2,3</sup>.

The relationship between Ruland's isotropic lattice disorder parameter and the root-mean-squared lattice strain clearly indicates thermal lattice vibrations and

lattice distortions of the first kind as the major source of cellulose lattice disorder at room temperature corresponding to similar findings in the case of synthetic polymers.

## ACKNOWLEDGEMENT

The authors are greatly indebted to Dr E. Walenta for valuable discussions.

## REFERENCES

- 1 Jayme, G., Raffael, E. and Islam, M. A. *Papier* 1973, **27**, 589
- 2 Fink, H.-P., Fanter, D. and Philipp, B. *Acta Polym.* 1985, **36**, 1
- 3 Fink, H.-P. and Philipp, B. *J. Appl. Polym. Sci.* 1985, **30**, 3779
- 4 Lenz, J., Schurz, J., Wrentschur, E. and Geymayer, W. *Angew. Makromol. Chem.* 1986, **138**, 1
- 5 Hindeleh, A. M. and Johnson, D. J. *Polymer* 1974, **15**, 697
- 6 Hindeleh, A. M., Johnson, D. J. and Montague, P. E. in 'Fiber Diffraction Methods', ACS Symp. Ser. 141, American Chemical Society, Washington DC, 1980, p. 149
- 7 Krässig, H. *Lenz. Ber.* 1977, **43**, 141
- 8 Kulshreshtha, A. K., Dweltz, N. E. and Radhakrishnan, T. J. *Appl. Crystallogr.* 1971, **4**, 116
- 9 Haase, J., Hosemann, R. and Renwanz, B. *Kolloid-Z. Z. Polym.* 1973, **251**, 871
- 10 Haase, J., Hosemann, R. and Renwanz, B. *Colloid Polym Sci.* 1974, **252**, 712
- 11 Haase, J., Hosemann, R. and Renwanz, B. *Cellulose Chem. Technol.* 1975, **9**, 513
- 12 Haase, J., Hosemann, R. and Renwanz, B. *Colloid Polym. Sci.* 1976, **254**, 199
- 13 Delhez, R., de Keijser, Th. H. and Mittemeijer, E. J. *Fresenius Z. Anal. Chem.* 1982, **312**, 1
- 14 Hofmann, D. and Walenta, E. *Polymer* 1987, **28**, 1271
- 15 Ruland, W. *Acta Crystallogr.* 1961, **14**, 1180
- 16 Vonk, C. G. J. *Appl. Crystallogr.* 1973, **6**, 148
- 17 Keating, D. T. *Rev. Sci. Instrum.* 1959, **30**, 725
- 18 Meyer, K. H. and Misch, L. *Helv. Chim. Acta* 1937, **20**, 232
- 19 Heuvel, H. M., Huisman, R. and Lind, K. C. J. B. *J. Polym. Sci., Polym. Phys. Edn.* 1976, **14**, 921
- 20 Stokes, A. R. *Proc. Phys. Soc. Lond. (A)* 1948, **61**, 382
- 21 Warren, B. E. and Averbach, B. L. *J. Appl. Phys.* 1950, **21**, 595
- 22 Warren, B. E. and Averbach, B. L. *J. Appl. Phys.* 1952, **23**, 497
- 23 Hosemann, R. and Bagchi, S. N. 'Direct Analysis of Diffraction by Matter', North-Holland, Amsterdam, 1962
- 24 Hosemann, R., Lemm, K., Schönfeld, A. and Wilke, W. *Kolloid-Z. Z. Polym.* 1967, **216**, 103
- 25 Warren, B. E. *Prog. Metall. Phys. (B)* 1959, **18**, 147
- 26 Buchanan, D. R., McCullough, R. L. and Miller, R. L. *Acta Crystallogr.* 1966, **20**, 922
- 27 Hosemann, R., Vogel, W., Weike, D. and Baltà Callea, F. J. *Acta Crystallogr. (A)* 1981, **37**, 85
- 28 Mignot, J. and Rondot, D. *Acta Metall.* 1975, **23**, 1321
- 29 Rothman, R. L. and Cohen, J. B. *J. Appl. Phys.* 1971, **24**, 971
- 30 Hosemann, R. and Hentschel, M. P. *Cellulose Chem. Technol.* 1985, **19**, 459
- 31 Kakudo, M. and Kasai, N. 'X-Ray Diffraction by Polymers', Kodansha, Tokyo, 1972